Journal of Materials Chemistry A

COMMUNICATION

View Article Online
View Journal | View Issue

Cite this: J. Mater. Chem. A, 2014, 2, 14812

Received 11th May 2014
Accepted 18th July 2014

DOI: 10.1039/c4ta02368d

www.rsc.org/MaterialsA

Template-assisted synthesis of CoP nanotubes to efficiently catalyze hydrogen-evolving reaction†

Hongfang Du,[ab] Qian Liu,[b] Ningyan Cheng,[b] Abdullah M. Asiri,[c] Xuping Sun*[bc] and Chang Ming Li*[a]

For the first time, we demonstrate a template-assisting synthesis to make CoP nanotubes (CoP NTs) through low-temperature phosphidation of Co salt inside a porous anodic aluminium oxide template followed by dilute HF etching. Such CoP NTs exhibit excellent hydrogen-evolution catalytic activity and durability in an acidic medium, which is superior to their nanoparticle counterparts, with a Faradaic yield of nearly 100%. The fundamental insight for the catalytic enhancement mechanism is also explored.

Depletion of fossil fuels and increased environmental concerns have prompted an urgent search for clean and sustainable alternative energy sources.[1] Hydrogen is a promising and green chemical fuel for future energy applications.[2] Electrolysis of water is a simple way to produce hydrogen with high purity, but an efficient hydrogen evolution reaction (HER) electrocatalyst is usually required to achieve high current density at low overpotential. Platinum, as the best HER catalyst, suffers from terrestrial scarcity and high cost.[3] Proton exchange membrane (PEM) technology uses highly acidic conditions, thus acid-stable HER catalysts are required in PEM-based electrolysis units.[4] Although there are some available HER catalysts, such as nickel or nickel-based alloy[5] working in alkaline solution, their long-term stability in strong acid condition needs significant improvement. Thus, considerable research effort has been paid to develop acid-stable non-noble metal HER catalysts, among which, the metal Mo-based compounds, such as MoS_2, MoS_x, $MoSo_y$/RGO, MoS_2/MoO_3, $MoSe_2$, $MoSe_2$/RGO, MoB, Mo_2C, Mo_2C/XC, $NiMoN_x$ and $Co_{0.6}Mo_{1.4}N_2$,[6] *etc.*, have received particular attention, and great progress has been achieved in the past years.

An ideal HER electrocatalyst should feature five prominent attributes, including nanoscale dimension to maximize the number of exposed active sites, high aspect ratio to improve catalytic activity per geometric area, porous structure to enhance fast mass transport of reactants and products,[6c] good electrical conductivity to facilitate electronic transfer[7] and unique physicochemical nature to give it high intrinsic catalytic[8] activity towards HER. Transition metal phosphides (TMPs) are formed from the alloying of metals and phosphorus with good electrical conductivity.[9] They have been widely used as catalysts for hydrodesulfurization (HDS) and hydrodenitrogenation (HDN).[9,10] Both HDS and HER rely on reversible binding of catalyst and hydrogen, with hydrogen dissociation to yield H_2S in HDS, while protons bound to the catalyst promote hydrogen evolution in HER.[11] Therefore, TMPs could serve as active catalysts towards HER. Indeed, previous work has shown that Ni_2P nanoparticles and FeP nanosheets catalyze electrochemical generation of hydrogen from water.[12] CoP hollow nanoparticles have also been developed as an effective HER catalyst,[13] but the catalyst preparation suffers from the involvement of several kinds of organic solvents and multiple tedious steps.

Herein, we report an organic solvent-free method for the synthesis of CoP nanotubes (CoP NTs). It was prepared *via* low-temperature phosphidation of Co salt inside a porous anodic aluminum oxide (AAO) template. It has been reported[14] that cobalt phosphide is stable in acids except in a mixture of nitric and hydrofluoric acid. Thus, CoP NTs can be obtained by etching the template with dilute HF solution. The as-prepared CoP NTs are used as a HER electrocatalyst in an acidic electrolyte with excellent activity and durability superior to CoP nanoparticles (CoP NPs). The Faradaic yield (FY) for hydrogen production is close to 100%.

The X-ray diffraction (XRD) patterns of CoP NTs and CoP NPs (see Experimental section for preparation details) are shown in

[a]Institute for Clean Energy & Advanced Materials, Faculty for Materials and Energy, Southwest University, Chongqing 400715, China. E-mail: ecmli@swu.edu.cn; Fax: +86 023-68254969

[b]State Key Lab of Electroanalytical Chemistry, Changchun Institute of Applied Chemistry, Chinese Academy of Sciences, Changchun 130022, Jilin, China. E-mail: sunxp@ciac.ac.cn; Fax: +86 431-85262065

[c]Chemistry Department, Faculty of Science, King Abdulaziz, University, Jeddah 21589, Saudi Arabia

† Electronic supplementary information ESI available: Experimental detail, additional information XPS and Table S1. See DOI: 10.1039/c4ta02368d

Fig. 1a. Both samples present characteristic diffraction peaks of CoP (JCPDS no. 65-1474). Fig. 1b shows the low magnification transmission electron microscopy (TEM) image of CoP NTs, indicating the formation of a large amount of one-dimensional (1D) nanostructures. The high magnification TEM image (Fig. 1c) clearly reveals its tubular nature. The formation of nanotubes is further verified by scanning TEM (STEM) observation as shown in Fig. 1d. The high resolution TEM (HRTEM) image captured from a single nanotube (Fig. 1e) reveals clear lattice fringes with an interplane distance of 0.189 nm corresponding to the (211) plane of CoP.[15] The energy dispersive X-ray (EDX) elemental mapping images of Co and P for CoP NTs show that both Co and P elements are uniformly distributed throughout the nanotubes, as shown in Fig. 1f. All these observations strongly confirm the successful synthesis of CoP NTs. However, it is noteworthy that the same preparation without the use of AAO template only produces CoP NPs (Fig. 1g).

We examined the HER catalytic performance of CoP NTs in 0.5 M H_2SO_4 electrolyte using a typical three-electrode setup. For comparison, bare GCE, CoP NPs and commercially available Pt/C (20 wt%) with the same loading were also studied. A saturated calomel electrode (SCE) reference electrode was used but was calibrated by a reversible hydrogen electrode (RHE) using a Pt foil immersed in 0.5 M H_2SO_4 saturated with high purity hydrogen before each electrochemical measurement, and all potentials in this work are reported *versus* RHE. Compensation of ohmic losses was performed for all electrochemical measurements. Fig. 2a shows the polarization curves of CoP NTs, CoP NPs, Pt/C and bare GCE. The Pt/C catalyst exhibits expected HER activity with a near zero overpotential while the bare GCE does not affect activity towards HER. It is clearly observed that CoP NTs have a much more rapid rise of cathodic currents than CoP NPs when the potential turns more negative. In addition, to achieve current densities of 2 and 10 mA cm^{-2}, the former needs overpotentials of only 72 and 129 mV, respectively, but the latter requires overpotentials of 200 and 297 mV, respectively. These results indicate that CoP NTs catalyst has much higher electroactivity toward HER. The performance achieved by our catalyst in an acidic electrolyte is much better than that of reported Mo-based catalysts, including double-gyroid MoS_2,[6c] metallic MoS_2 nanosheets,[6d] MoS_3 particles,[6f] MoS_2/MoO_3,[6h] bulk MoB,[6j] Mo_2C nanocrystals,[6k] $MoSe_2$/RGO,[6l] $NiMoN_x$,[6o] $Co_{0.6}Mo_{1.4}N_2$.[6p] Our catalyst is also better than FeP nanosheets[12c] and TaCN nanoparticle,[16] whose values are shown in Table S1.†

Fig. 2b shows the Tafel plots of CoP NTs, CoP NPs and Pt/C. The linear regions of the Tafel plots were fit to the Tafel

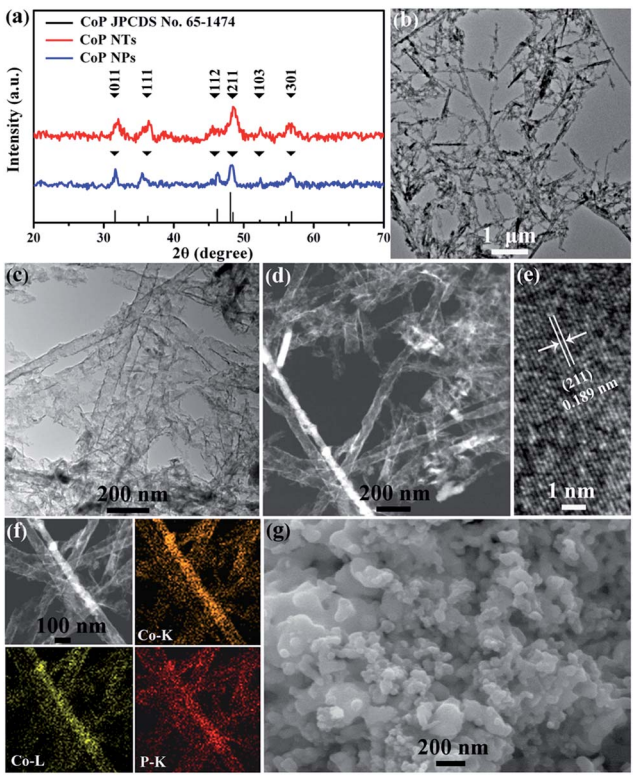

Fig. 1 (a) XRD patterns of CoP NTs and CoP NPs. (b) Low and (c) high magnification TEM images of CoP NTs. (d) STEM image of CoP NTs. (e) HRTEM image of CoP NTs. (f) EDX elemental mapping images of Co and P for CoP NTs. (g) Typical SEM image of CoP NPs.

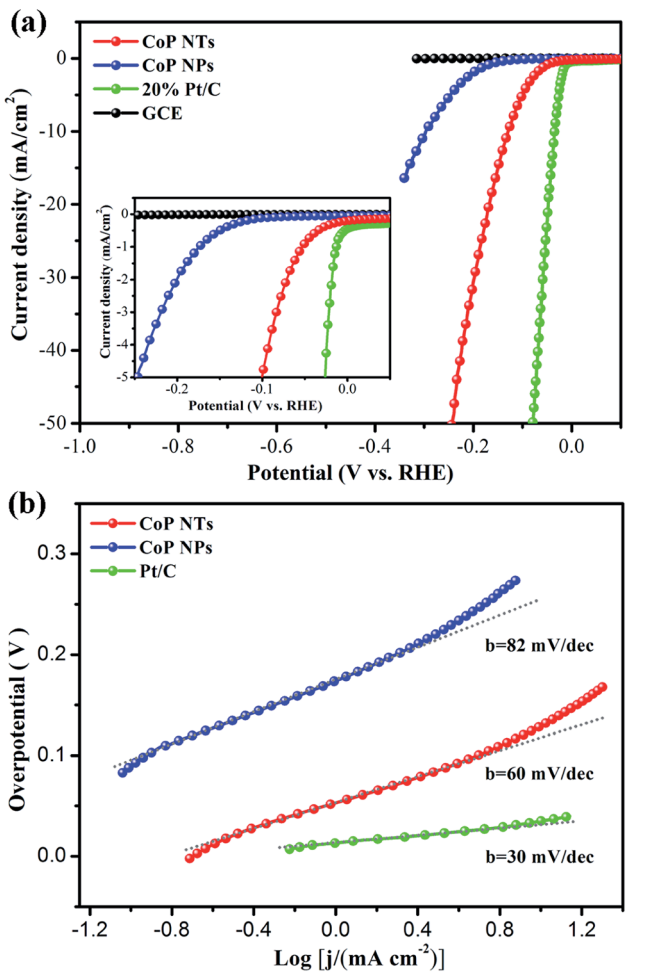

Fig. 2 (a) Polarization curves of CoP NTs, CoP NPs, Pt/C and bare GCE. (b) Tafel plots of CoP NTs, CoP NPs and Pt/C.

equation ($\eta = b \log j + a$, where j is the current density and b is the Tafel slope), yielding Tafel slopes of 60, 82 and 30 mV per dec for CoP NTs, CoP NPs and Pt/C catalyst, respectively. The Tafel slope of CoP NTs is smaller than that of some non-noble metal catalysts like bulk MoS_2 (94 mV per dec),[6b] amorphous MoS_2 (60 mV per dec),[6e] $MoSo_y$/RGO (62.7 mV per dec),[6g] bulk Mo_2C (87.6 mV per dec),[6j] Mo_2C nanocrystals (110–235 mV per dec),[6k] $MoSe_2$/RGO (101 mV per dec),[6l] TaCN nanoparticles (103–158 mV per dec)[15] and NiSe nanofiber assemblies (64 mV per dec).[17] It is also comparable to that of MoO_3/MoS_2 nanowires (50–60 mV per dec)[6h] and Mo_2C/XC (59.4 mV per dec)[6m] *etc.* Tafel slopes of 30, 40 and 120 mV per dec can be achieved if the Tafel, Heyrovsky or Volmer step is the rate-determining step, respectively.[18] The experimentally observed Tafel slopes of 60 and 82 mV per dec for CoP NTs and CoP NPs reveal that the Volmer–Heyrovsky HER mechanism presumably takes effect in the HER, and the electrochemical desorption is the rate-limiting step.[6b]

We further probed the durability of CoP NTs and CoP NPs in an acidic medium by a long-term cycling test. Fig. 3a shows the comparison of polarization curves measured before and after 3000 cyclic voltammetry (CV) cycles ranging from −0.2 to 0.2 V at a scan rate of 100 mV s^{-1}. At the end of cycling, only negligible current loss is observed in the polarization curves of CoP NTs. However, CoP NPs shows obvious current loss up to 3000 cycles. Fig. 3b shows the time-dependent current density curves of CoP NTs and CoP NPs under static overpotential of 150 mV. After a long period of 30000 s, around 80% of the current intensity for CoP NTs can still be maintained, but only 45% for CoP NPs is maintained. These observations indicate that CoP NTs have superior stability in a long-term electrochemical process over CoP NPs.

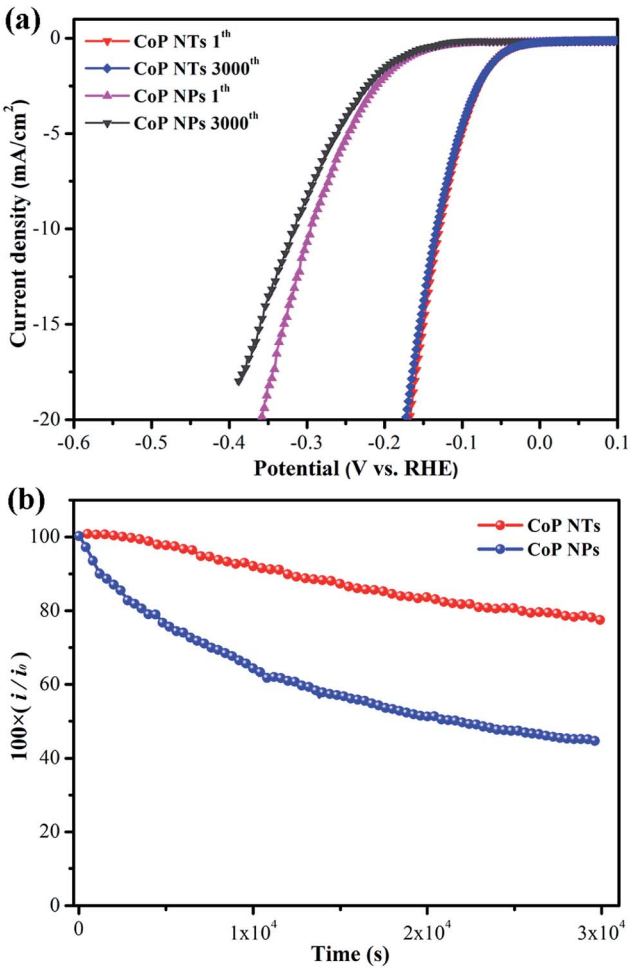

Fig. 3 (a) Polarization curves of CoP NTs and CoP NPs initially and after 3000 CV scans between −0.2 and +0.2 V. (b) Time-dependent current density curves of CoP NTs and CoP NPs under static overpotential of 150 mV.

To gain further insights into the intrinsic catalytic activity of CoP NTs and CoP NPs, turnover frequency (TOF) for each active site was estimated using the reported methods.[19] The number of active sites was examined by CVs at a scan rate of 50 mV s^{-1} over a range of −0.2 to 0.8 V in phosphate buffer (pH = 7) (Fig. S1†). No apparent redox peak was observed, indicating one electron transfer process, and thus, the integrated charge over the entire potential range should be proportional to the total number of active sites. The calculated number of the active sites for CoP NTs and CoP NPs are 3.79×10^{-9} and 1.60×10^{-10} mol, respectively. Fig. 4 shows the polarization curves (measured in 0.5 M H_2SO_4) normalized by the active sites and expressed in terms of TOF. To accomplish a TOF value of 1.00 s^{-1}, CoP NTs and CoP NPs need overpotentials of 106 and 172 mV, respectively. The TOF value of CoP NTs is comparable to that of the several reported non-noble metal-based catalysts.[12a,20] The superior catalytic performance of the CoP NTs catalyst could be attributed to its 1D tubular nanostructure. On one hand, the high aspect ratio of CoP NTs effectively improves catalytic activity per geometric area;[6c] on the other hand, both the inner and outer surface of CoP NTs can be accessed by electrolyte, thus providing more exposed active sites.

MoP has recently been reported to possess better catalytic ability than Mo_3P towards HER due to more favorable H-binding on P sites of MoP,[21] indicating that catalytic ability of molybdenum phosphide is strongly affect by its constitution.

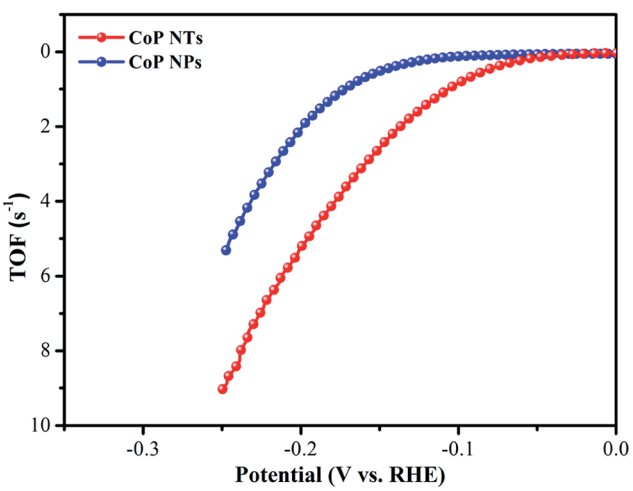

Fig. 4 Calculated TOFs for CoP NTs and CoP NPs in 0.5 M H_2SO_4.

We can also reasonably expect that cobalt phosphide could have a similar constitution effect on its catalytic ability towards HER. Fig. S2† shows the X-ray photoelectron spectroscopy (XPS) 2p spectra in the Co (2p) and P (2p) regions of CoP NTs. One obvious peak appears at 779.1 eV in the Co (2p) region along with two peaks at 134.0 and 129.9 eV in the P (2p) region. The observed two peaks at 779.1 and 129.9 eV confirm the formation of CoP.[22] The peak at 134.0 eV in the P (2p) can be assigned to oxidized species arising from superficial oxidation due to air contact.[23] The positive shift of Co (2p) binding energy (779.1 eV) from Co metal (778.1–778.2 eV) and the negative shift of P (2p) binding energy (129.9 eV) from elemental P (130.2 eV)[24] suggest that the Co and P in CoP have a partial positive and negative charge, respectively, which result from the transfer of electron density from Co to P.[25] Indeed, calculations and electron density maps also suggest covalency for Co–P bonds with charge separation due to charge transfer from Co to P.[26] It is known that metal complex HER catalysts incorporate proton relays from pendant acid-base groups positioned close to the metal activation center where H_2 production occurs,[27] and hydrogenases also use pendant bases proximate to the metal centers as active sites.[28] Considering that CoP also features a pendant base P in close proximity to the metal Co, we may expect it to share similar catalytic mechanism with metal complex catalysts and hydrogenases toward the HER.

We further confirmed the gas generation by gas chromatography (GC) for a quantitative measurement of the generated hydrogen, in which a calibrated pressure sensor is used to monitor the pressure change in the cathode compartment of an H-type electrolytic cell. Bulk cathodic electrolysis was carried out by maintaining CoP NTs-loaded glassy carbon plate under a static overpotential of 250 mV for a period of time. To calculate the FY of the electrocatalytic hydrogen evolution, we compared the amount of experimentally quantified hydrogen with theoretically calculated hydrogen (assuming 100% FY) as shown in Fig. 5. The result suggests that the CoP NPs have FY of nearly 100%.

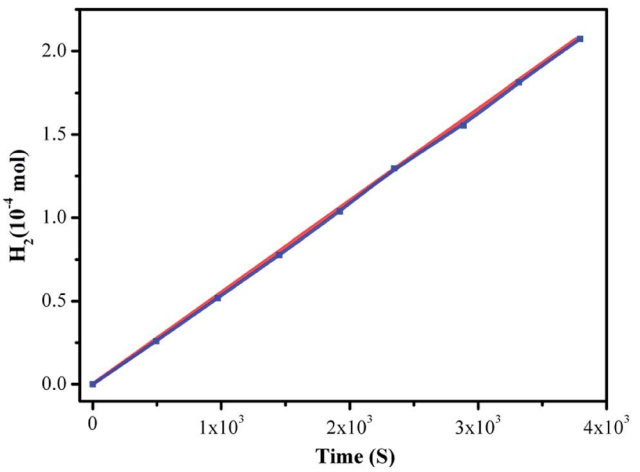

Fig. 5 Amount of theoretically calculated (red) and experimentally measured (green) hydrogen *versus* time of CoP NTs under a static overpotential of 250 mV.

In summary, CoP NTs have been successfully synthesized *via* the low-temperature phosphidation of Co salt inside a porous AAO template followed by dilute HF etching. Such CoP NTs as a novel HER catalyst show excellent activity and durability in an acidic medium with a FY close to 100%. This work provides a general methodology to fabricate nanotubes of TMP for applications toward electrocatalysis and Li-ion batteries.[9,10]

Acknowledgements

This work was supported by the National Natural Science Foundation of China (no. 21175129) and the National Basic Research Program of China (no. 2011CB935800). We would also like to gratefully acknowledge the financial support from Chongqing Key Laboratory for Advanced Materials and Technologies of Clean Energies, Start-up grant under SWU111071 from Southwest University.

Notes and references

1 (*a*) A. J. Bard and M. A. Fox, *Acc. Chem. Res.*, 1995, **28**, 141; (*b*) J. Liu, G. Liu, M. Li, W. Shen, Z. Liu, J. Wang, J. Zhao, L. Jiang and Y. Song, *Energy Environ. Sci.*, 2010, **3**, 1503.

2 (*a*) M. S. Dresselhaus and I. L. Thomas, *Nature*, 2001, **414**, 332; (*b*) J. A. Turner, *Science*, 2004, **305**, 972; (*c*) H. B. Gray, *Nat. Chem.*, 2009, **1**, 7.

3 M. G. Walter, E. L. Warren, J. R. McKone, S. W. Boettcher, Q. X. Mi, E. A. Santori and N. S. Lewis, *Chem. Rev.*, 2010, **110**, 6446.

4 (*a*) G. A. Le, V. Artero, B. Jousselme, P. D. Tran, N. Guillet, R. Métayé, A. Fihri, S. Palacin and M. Fontecave, *Science*, 2009, **326**, 1384; (*b*) B. C. Steele and A. Heinzel, *Nature*, 2001, **414**, 345.

5 (*a*) S. H. Ahn, S. J. Hwang, S. J. Yoo, I. Choi, H. J. Kim, J. H. Jang, S. W. Nam, T. H. Lim, T. Lim and S. K. Kim, *J. Mater. Chem.*, 2012, **22**, 15153; (*b*) M. P. Kaninski, D. P. Saponjic, V. M. Nikolic, D. L. Zugic and G. S. Tasic, *Int. J. Hydrogen Energy*, 2011, **36**, 8864; (*c*) Q. Han, S. Cui, N. Pu, J. Chen, K. Liu and X. Wei, *Int. J. Hydrogen Energy*, 2010, **35**, 5194.

6 For example, see: (*a*) T. F. Jaramillo, K. P. Jørgensen, J. Bonde, J. H. Nielsen, S. Horch and I. Chorkendorff, *Science*, 2007, **317**, 100; (*b*) Y. Li, H. Wang, L. Xie, Y. Liang, G. Hong and H. Dai, *J. Am. Chem. Soc.*, 2011, **133**, 7296; (*c*) J. Kibsgaard, Z. Chen, B. N. Reinecke and T. F. Jaramillo, *Nat. Mater.*, 2012, **11**, 963; (*d*) M. A. Lukowski, A. S. Daniel, F. Meng, A. Forticaux, L. Li and S. Jin, *J. Am. Chem. Soc.*, 2013, **135**, 10274; (*e*) J. D. Benck, Z. B. Chen, L. Y. Kuritzky, A. J. Forman and T. F. Jaramillo, *ACS Catal.*, 2012, **2**, 1916; (*f*) H. Vrubel, D. Merki and X. Hu, *Energy Environ. Sci.*, 2011, **5**, 6136; (*g*) W. Chen, S. Iyer, S. Iyer, K. Sasaki, C. Wang, Y. Zhu, J. T. Muckerman and E. Fujita, *Energy Environ. Sci.*, 2013, **6**, 1818; (*h*) Z. Chen, D. Cummins, B. N. Reinecke, E. Clark, M. K. Sunkara and T. F. Jaramillo, *Nano Lett.*, 2011, **11**, 4168; (*i*) D. Kong, H. Wang, J. J. Cha, M. Pasta, K. J. Koski, J. Yao and Y. Cui, *Nano Lett.*, 2013, **13**, 1341; (*j*) H. Vrubel and X. Hu, *Angew. Chem. Int. Ed.*,

2012, **54**, 12703; (*k*) N. S. Alhajri, D. H. Anjum and K. Takanabe, *J. Mater. Chem. A*, 2014, **2**, 10548; (*l*) H. Tang, K. Dou, C. C. Kaun, Q. Kuang and S. Yang, *J. Mater. Chem. A*, 2014, **2**, 360; (*m*) W. Chen, C. Wang, K. Sasaki, N. Marinkovic, W. Xu, J. T. Muckerman, Y. Zhu and R. R. Adzic, *Energy Environ. Sci.*, 2013, **6**, 943; (*n*) L. Liao, S. Wang, J. Xiao, X. Bian, Y. Zhang, M. D. Scanlon, X. Hu, Y. Tang, B. Liu and H. H. Girault, *Energy Environ. Sci.*, 2014, **7**, 387; (*o*) W. Chen, K. Sasaki, C. Ma, A. I. Frenkel, N. Marinkovic, J. T. Muckerman, Y. Zhu and R. R. Adzic, *Angew. Chem., Int. Ed.*, 2012, **51**, 6131; (*p*) B. Cao, G. M. Veith, J. C. Neuefeind, R. R. Adzic and P. G. Khalifah, *J. Am. Chem. Soc.*, 2013, **135**, 19186.

7 Y. Fu, Z. Yang, X. Li, X. Wang, D. Liu, D. Hu, L. Qiao and D. He, *J. Mater. Chem. A*, 2013, **1**, 10002.

8 I. L. C. Buurmans, J. Ruiz-Martínez, W. V. Knowles, D. van der Beek, J. A. Bergwerff, E. T. Vogt and B. M. Weckhuysen, *Nat. Chem.*, 2011, **3**, 862.

9 S. T. Oyama, T. Gott, H. Zhao and Y. K. Lee, *Catal. Today*, 2009, **143**, 94.

10 (*a*) S. Carenco, D. Portehault, C. Boissière, N. Mèzailles and C. Sanchez, *Chem. Rev.*, 2013, **113**, 7981; (*b*) R. Prins and M. E. Bussell, *Catal. Lett.*, 2012, **142**, 1413.

11 (*a*) J. O. M. Bockris and E. C. Potter, *J. Electrochem. Soc.*, 1952, **99**, 169; (*b*) P. Liu and J. A. Rodriguez, *J. Am. Chem. Soc.*, 2005, **127**, 14871.

12 (*a*) E. J. Popczun, J. R. McKone, C. G. Read, A. J. Biacchi, A. M. Wiltrout, N. S. Lewis and R. E. Schaak, *J. Am. Chem. Soc.*, 2013, **135**, 9267; (*b*) L. Feng, H. Vrubel, M. Bensimon and X. Hu, *Phys. Chem. Chem. Phys.*, 2014, **16**, 5917; (*c*) Y. Xu, R. Wu, J. Zhang, Y. Shi and B. Zhang, *Chem. Commun.*, 2013, **49**, 6656.

13 J. Popczun, C. G. Read, C. W. Roske, N. S. Lewis and R. E. Schaak, *Angew. Chem., Int. Ed.*, 2014, **53**, 5427.

14 G. Maronneau, *Compt. Rend. (Paris)*, 1900, **130**, 656.

15 W. Maneeprakorn, M. A. Malik and P. O'Brien, *J. Mater. Chem.*, 2010, **20**, 2329.

16 N. S. Alhajri, H. Yoshida, D. H. Anjum, A. T. Garcia-Esparza, J. Kubota, K. Domen and K. Takanabe, *J. Mater. Chem. A*, 2013, **1**, 12606.

17 M. Gao, Z. Lin, T. Zhuang, J. Jiang, Y. Xu, Y. Zheng and S. Yu, *J. Mater. Chem.*, 2012, **22**, 13662.

18 W. Chen, J. T. Muckerman and E. Fujita, *Chem. Commun.*, 2013, **49**, 8896.

19 D. Merki, S. Fierro, H. Vrubel and X. Hu, *Chem. Sci.*, 2011, **2**, 1262.

20 (*a*) J. R. McKone, B. F. Sadtler, C. A. Werlang, N. S. Lewis and H. B. Gray, *ACS Catal.*, 2013, **3**, 166; (*b*) J. Xie, H. Zhang, S. Li, R. Wang, X. Sun, M. Zhou, J. Zhou, X. Lou and Y. Xie, *Adv. Mater.*, 2013, **25**, 807.

21 P. Xiao, M. A. Sk, L. Thia, X. Ge, R. J. Lim, J. Y. Wang, K. H. Lim and X. Wang, *Energy Environ. Sci.*, 2014, **7**, 2624.

22 A. P. Grosvenor, S. D. Wik, R. G. Cavell and A. Mar, *Inorg. Chem.*, 2005, **44**, 8988.

23 (*a*) S. Carenco, C. Surcin, M. Morcrette, D. Larcher, N. Mézailles, C. Boissière and C. Sanchez, *Chem. Mater.*, 2012, **24**, 688; (*b*) H. Li, P. Yang, D. Chu and H. Li, *Appl. Catal., A*, 2007, **325**, 34.

24 *Practical Surface Analysis by Auger and X-ray Photoelectron Spectroscopy*, ed. D. Briggs and M. P. Seah, John Wiley & Sons, New York, 1983.

25 A. W. Burns, K. A. Layman, D. H. Bale and M. E. Bussell, *Appl. Catal., A*, 2008, **343**, 68.

26 S. Diplas, Ø. Prytz, O. B. Karlsen, J. Fwatts and J. Taftø, *J. Phys.: Condens. Matter*, 2007, **19**, 246216.

27 (*a*) A. D. Wilson, R. H. Newell, M. J. McNevin, J. T. Muckerman, M. R. Dubois and D. L. Dubois, *J. Am. Chem. Soc.*, 2006, **128**, 358; (*b*) A. D. Wilson, R. K. Shoemaker, A. Miedaner, J. T. Muckerman, D. L. Dubois and M. R. Dubois, *Proc. Natl. Acad. Sci. U. S. A.*, 2007, **104**, 6951; (*c*) B. E. Barton and T. B. Rauchfuss, *J. Am. Chem. Soc.*, 2010, **132**, 14877.

28 Y. Nicolet, A. L. de Lacey, X. Vérnede, V. M. Fernandez, E. C. Hatchikian and J. C. Fontecilla-Camps, *J. Am. Chem. Soc.*, 2001, **123**, 1596.

